Journal of Inorganic and General Chemistry
ZAAC
Zeitschrift für anorganische und allgemeine Chemie
www.zaac.wiley-vch.de
RESEARCH ARTICLE
Check for updates
DOI: 10.1002/zaac.202200257

# Synthesis and Crystal Structures of a Series of Five [M{$Me_2Si(NPh)_2$}$L_2$] Complexes (M = Cr, Mn, Fe, Co, Zn) With NHC Co-ligands

Christian Heiser[a] and Kurt Merzweiler*[a]

A series of five M(II) silylamide complexes [M{$Me_2Si(NPh)_2$}($^i Pr_2Im$)$_2$] (M = Cr, Mn, Fe, Co, Zn), $^i Pr_2Im$ = 1,3-diisopropylimidazoline-2-ylidene) were synthesized and characterized by spectroscopic methods and single crystal X-ray analyses. The Cr(II) complex [Cr{$Me_2Si(NPh)_2$}($^i Pr_2Im$)$_2$] exhibits a distorted square planar coordination from a chelating $Me_2Si(NPh)_2$ group and two NHC ligands. In the case of the Mn, Fe, Co and Zn derivatives the coordination mode is distorted tetrahedral. With exception of the Zn complex all derivatives are paramagnetic with $\mu_{eff.}$ values of 4.71 B.M. (Cr), 5.08 B.M. (Fe), 5.91 B.M. (Mn) and 3.94 B.M. (Co).

## Introduction

Silylamido ligands of the type $R_2Si(NR')_2^{2-}$ have found widespread application in main group and transition metal chemistry.[1] In the beginnings some 40 years ago, research in this field mainly focused on Ti(IV), Zr(IV), Hf(IV) and V(IV) complexes of the type [M{$R_2Si(NR')_2$}$_2$].[2,3,4] These compounds are easily accessible from the reaction of metal tetrahalides and the appropriate lithium silylamides $Li_2R_2Si(NR')_2$ in 1:2 molar ratio. In [M{$R_2Si(NR')_2$}$_2$] complexes the presence of two double negatively charged silylamide ligands balances the 4+ charge of the metal center and moreover ensures its coordinative saturation. Thus, the formation of monomeric species is strongly favored, particularly in the case of the bulky N$^t$Bu residues. More recently, an analogous Co(IV) complex [Co{$Me_2Si(N^tBu)_2$}$_2$] was obtained from [$CoCl_2$(TMEDA)] and $Li_2Me_2Si(N^tBu)_2$ including a disproportionation reaction.[5] Moving to silylamides of monovalent M(I) or divalent M(II) transition metals, the situation turns more complex as monomeric species [M(I)$_2${$R_2Si(NR')_2$}] and [M(II){$R_2Si(NR')_2$}] would contain coordinatively unsaturated metal sites and – in absence of suitable co-ligands – the formation of polynuclear complexes is to be expected. This is especially true for Cu(I) silylamides [$Cu_2R_2Si(NPh)_2$] that exist as tetramers like [$Cu_8${$R_2Si(NPh)_2$}$_4$] (R = Me, Ph).[6] Moreover, the employment of auxiliary donor ligands allows for the generation of monomeric complex species, like in the case of [$Cu_2${$Me_2Si(N$-$C_6H_4$-2-$SPh)_2$($PMe_3$)$_2$}].[7] Currently, there are only few reports on complexes of divalent transition metals M(II) with difunctional silylamido ligands. One of the first reports came from P.P. Power *et al.* who described the synthesis of the dinuclear Mn(II) complex Li[$Mn_2${$Me_2Si(NMes)_2$}$_2${$N(SiMe_3)_2$}] in 1991.[8] In particular in the case of Mn(II), Zn(II), Cd(II)[9] and Mo(II)[10] the application of the sterically encumbered $Me_2Si(NDipp)_2^{2-}$ ligand has proven to be most effective for the synthesis of dinuclear complexes of the type [M(II)$_2${$Me_2Si(NDipp)_2$}$_2$]. Additionally, there are some recent reports on anionic chelate complexes of the type [RM{$Ph_2Si(NDipp)_2$}$_2$]$^-$ with R = $N(SiMe_3)_2$, $CH_2SiMe_3$, M = Zn[11] and M = Mn.[12] Furthermore, a pyridyl functionalized silylamido ligand was successfully used for the synthesis of the trinuclear Fe(II) complex [$Fe_3${$Me_2Si(N$-$CH_2$-*o*-$py)_2$}$_2$$Cl_2$][13] and a 8-quinolyl functionalized silylamine led to a dinuclear Zn(II) complex [$Zn_2${$Ph_2Si(NR')_2$}$_2$] (R = 8-quinolyl).[14] Recently we reported on square planar Ni(II) complexes of the type [Ni{$R_2Si(N$-$C_6H_4$-2-$SR')_2$}] with R = Me and R' = *t*-Bu or R = Ph and R' = Me, Ph that contain tetradentate thioether functionalized silylamides in κ-*N,N',S,S'*coordination mode.[15] Within the course of these investigations we were interested in the coordination behavior of the non-functionalized silylamide ligand $Me_2Si(NPh)_2^{2-}$ towards a series of divalent transition metals, namely Cr(II), Mn(II), Fe(II), Co(II) and Zn(II). In order to suppress further oligomerization of the M(II) silylamides, the syntheses were carried out in the presence of the NHC ligand 1,3-diisopropylimidazoline-2-ylidene ($^i Pr_2Im$).

## Results and Discussion

Treatment of a violet solution of chromium(II) acetate and $^i Pr_2Im$ in THF with a solution of $Li_2Me_2Si(NPh)_2$ in the same solvent at −70 °C led to the formation of a deeply red colored reaction mixture. After warming up to room temperature and stirring over night the solvent was removed under reduced pressure and the remaining solid was extracted with hot toluene. Storing

[a] C. Heiser, Prof. Dr. K. Merzweiler
Institut für Chemie
Naturwissenschaftliche Fakultät II
Universität Halle
Kurt-Mothes-Str. 2
06120 Halle
E-mail: kurt.merzweiler@chemie.uni-halle.de



 

the toluene extract at room temperature led to the precipitation of red microcrystalline [Cr{$Me_2Si(NPh)_2$}($^iPr_2Im$)$_2$] (**1**) which was isolated in 59% yield (Scheme 1). Similar procedures starting from [M(acac)$_2$(TMEDA)]/$^iPr_2Im$ solutions and $Li_2Me_2Si(NPh)_2$ in THF as solvent were applied for the preparation of the [M{$Me_2Si(NPh)_2$}($^iPr_2Im$)$_2$] complexes (M = Mn (**2**), Fe (**3**), Co (**4**), Zn (**5**)) in yields around 60% (Scheme 1). The products were obtained as colorless (M = Mn, Zn), yellow (Fe) and green (Co) highly air- and moisture sensitive solids. The complexes are readily soluble in THF and less soluble in toluene and dimethoxyethane.

The IR spectra of compounds **1**–**5** clearly indicate the formation of the silyamide/NHC complexes by the absence of N–H vibrations and the presence of strong absorptions due to the silyamide part (1577, 1480, 1305 cm$^{-1}$) and the NHC ligands (2932, 1206, 927 cm$^{-1}$). Additionally $^1$H-NMR spectroscopy of the diamagnetic complex [Zn{$Me_2Si(NPh)_2$}($^iPr_2Im$)$_2$] (**5**) (in THF-$D_8$) confirmed the presence of the silylamide unit through the singlet signal of the $Me_2Si$ group at δ = 0.17 ppm and multiplet signals of the phenyl groups in the range 6.71–5.97 ppm. The signals of the $^iPr_2Im$ ligands consist of a singlet at 7.35 ppm for the imidazoline-2-ylidene group along with a septet (δ = 5.13 ppm) and doublet signals (δ = 1.23 ppm) for the iso-propyl groups. In the $^{13}$C NMR spectrum the signal of the carbene C atom of the $^iPr_2Im$ ligands appears at δ = 176.7 ppm. This corresponds to an upfield shift of 35.2 ppm with respect to the free 1,3-diisopropylimidazoline-2-ylidene (212.9 ppm). The $^{29}$Si NMR spectrum consists of a singlet signal at δ = −17 ppm. This corresponds to a slight upfield shift in comparison with the $^{29}$Si NMR resonances of $Me_2Si(NHPh)_2$,[16] [Li(OEt$_2$)$_3$][Ga{$Me_2Si(NPh)_2$}$_2$][17] and [{Li(OEt$_2$)}$_3$In{$Me_2Si(NPh)_2$}$_3$][17] that were observed around −11 ppm. By contrast, the $^{29}$Si NMR signal of [$Cu_8${$Me_2Si(NHPh)_2$}$_4$] appears at 17 ppm and exhibits a strong downfield shift.[6] Complexes **1**–**4** are paramagnetic. The determination of the magnetic moments of the solids gave the following values: [Cr{$Me_2Si(NPh)_2$}($^iPr_2Im$)$_2$] (**1**): 4.71 B.M., [Fe{$Me_2Si(NPh)_2$}($^iPr_2Im$)$_2$] (**2**): 5.08 B.M., [Mn{$Me_2Si(NPh)_2$}($^iPr_2Im$)$_2$] (**3**): 5.91 B.M. and [Co{$Me_2Si(NPh)_2$}($^iPr_2Im$)$_2$] (**4**): 3.94 B.M. which indicate high-spin electron configuration.

## Crystal structures

In order to get detailed insight into the molecular structures of complexes **1**–**5** X-ray single crystal determinations were carried out. Details of the data collection und structure refinements are collected in Table 1.

Dark red single crystals of the chromium(II) complex **1** were obtained by recrystallization from *o*-xylene. Compound **1** forms triclinic crystals, space group $P\bar{1}$. The unit cell contains two [Cr{$Me_2Si(NPh)_2$}($^iPr_2Im$)$_2$] units and two disordered molecules of *o*-xylene residing on a center of inversion. The molecular structure of the [Cr{$Me_2Si(NPh)_2$}($^iPr_2Im$)$_2$] complex (Figure 1) consists of a central chromium atom that is coordinated by the nitrogen atoms of a chelating $Me_2Si(NPh)_2$ unit and the carbon atoms of two $^iPr_2Im$ ligands. The coordination geometry can be described as distorted square planar. The Cr–N distances are 203.1(2) pm and 204.3(2) pm. Similar values were found in various [Cr{$N(SiMe_3)_2$}$_2$L$_2$] complexes with tetra-coordinate chromium atoms, e.g. [Cr{$N(SiMe_3)_2$(THF)$_2$] (Cr–N: 207.0(3) pm–207.8(3) pm),[18] [Cr{$N(SiMe_3)_2$(py)$_2$] (Cr–N: 204.0(3) pm–204.4(3) pm),[18] [Cr{$N(SiMe_3)_2$(bipy)] (Cr–N: 205.2(2) pm–205.7(2) pm)[19] and [Cr{$N(SiMe_3)_2$(TMEDA)] (Cr–N: 207.3(2)–208.0(2) pm).[20] The Cr–C distances are 214.4(2) pm and 214.6(2) pm. According to the CSD database[21] Cr–C separations in square planar Cr(II)-NHC complexes vary from 209.3 pm to 218.0 pm with a median value of 216.2 pm (17 data, lower quantile: 214.9 pm, upper quantile: 216.4 pm). Complex **1** exhibits a relatively small N–Cr–N angle of 76.0(1)°. Obviously, this is forced due to the formation of a four-membered $SiN_2Cr$

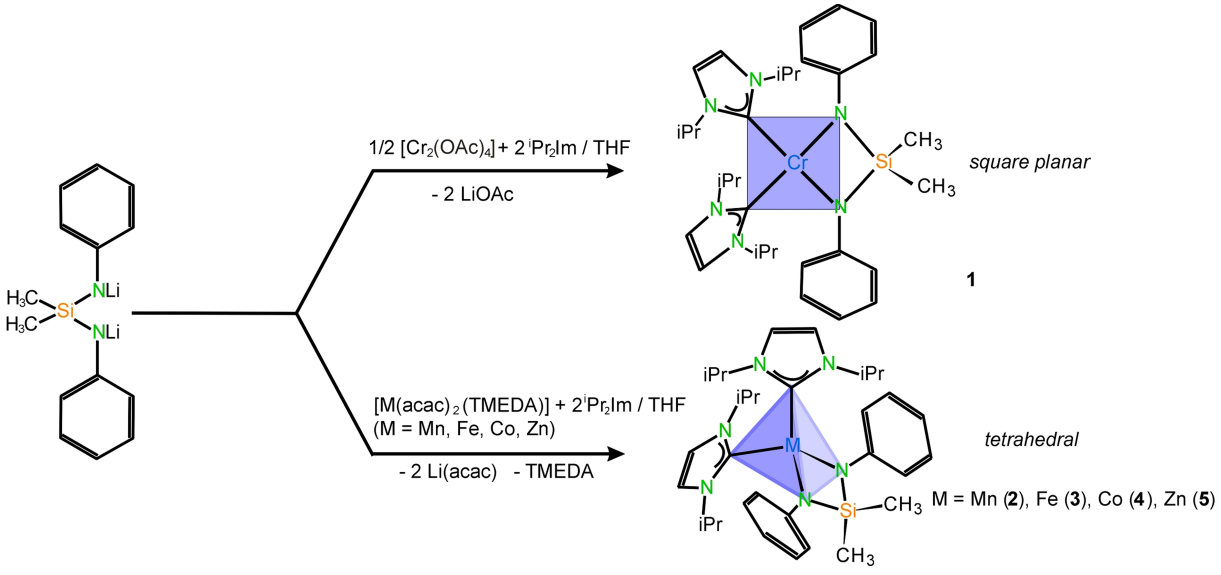


**Scheme 1.** Synthesis of the complexes [M{$Me_2Si(NPh)_2$}($^iPr_2Im$)$_2$] (M = Cr, Mn, Fe, Co, Zn).

 

**Table 1.** Crystallographic data and details of the crystal structure refinement for compounds **1**–**5**.

| | **1** | **2** | **3** | **4** | **5** |
|---|---|---|---|---|---|
| Empirical formula | $C_{32}H_{48}CrN_6Si{\cdot}C_8H_{10}$ | $C_{32}H_{48}MnN_6Si$ | $C_{32}H_{48}FeN_6Si$ | $C_{32}H_{48}CoN_6Si$ | $C_{32}H_{48}ZnN_6Si$ |
| Formula weight/g·mol$^{-1}$ | 703.01 | 599.79 | 600.70 | 603.78 | 610.22 |
| Temperature/K | 170 | 170 | 170 | 170 | 170 |
| Crystal system | Triclinic | Tetragonal | Tetragonal | Tetragonal | Tetragonal |
| Space group | $P\bar{1}$ | $P4_1$ | $P4_3$ | $P4_1$ | $P4_1$ |
| Unit cell dimensions/ pm/° | | | | | 1024.10(3) |
| a | 1137.88(5) | 1026.82(2) | 1026.80(2) | 1023.36(2) | |
| b | 1221.04(6) | 1026.82(2) | 1026.80(2) | 1023.36(2) | 1024.10(3) |
| c | 1542.57(7) | 3239.93(7) | 3229.4(1) | 3228.48(9) | 3221.35(12) |
| α | 84.417(4) | 90 | 90 | 90 | 90 |
| β | 82.883(4) | 90 | 90 | 90 | 90 |
| γ | 79.628(4) | 90 | 90 | 90 | 90 |
| Volume/nm$^3$ | 2.0858(2) | 3.4161(2) | 3.4048(2) | 3.3811(2) | 3.3785(2) |
| Z | 2 | 4 | 4 | 4 | 4 |
| Calculated density/ g·cm$^{-3}$ | 1.119 | 1.166 | 1.172 | 1.186 | 1.200 |
| Absorption coefficient μ/mm$^{-1}$ | 0.336 | 0.450 | 0.507 | 0.572 | 0.792 |
| Crystal size/mm$^3$ | 0.291×0.202×0.135 | 0.529×0.037×0.023 | 0.650×0.427×0.070 | 0.450×0.108×0.070 | 0.448×0.075×0.066 |
| Θ range for data collection/° | 1.700–29.242 | 2.348–26.838 | 1.983–26.754 | 1.990–26.723 | 1.989–26.800 |
| Reflections collected | 22993 | 11744 | 23738 | 25290 | 12217 |
| R(int) | 0.0382 | 0.0497 | 0.0660 | 0.0540 | 0.0540 |
| Data/restraints/ parameters | 11178/328/515 | 7100/1/371 | 7174/1/371 | 7134/1/371 | 7118/1/371 |
| Goodness-of-fit on F$^2$ | 1.014 | 1.190 | 1.039 | 1.064 | 0.999 |
| $R_1$ ($I > 2\sigma(I)$) | 0.0470 | 0.0531 | 0.0350 | 0.0282 | 0.0415 |
| $wR_2$ (all data) | 0.1326 | 0.1050 | 0.0844 | 0.0679 | 0.0963 |
| Flack Parameter[38] | | −0.013(17) | −0.001(15) | 0.007(6) | −0.030(12) |
| CCDC | 2179083 | 2179084 | 2179085 | 2179086 | 2179087 |

chelate ring. In contrast, the C–Cr–C angle (91.0(1)°) is much closer to the ideal value. Along with the N–Cr–C angles (95.14(7)–102.54(7)°/155.74(8)–166.94(8)°) the sum of the cis-angles around Cr is 364.7°. This indicates a moderate deviation from ideal square planar arrangement. The distortion may also be expressed by the $\tau_4'$ parameter[22] which amounts to 0.23. In the case of ideal square planar coordination the value of $\tau_4'$ would be zero. The Si–N bond lengths (170.9(2) and 172.8(2) pm) are comparable to those found in the parent amino silane $Me_2Si(NHPh)_2$ (172.2(2)–174.1(2) pm)[23] and several complexes like $[Yb\{Me_2Si(NPh)_2(Cp)_2\}^-$ (171.9(7)–172.9(5) pm),[24] $[Cu_8\{Me_2Si(NPh)_2\}_4]$ (174.9(3)–175.0(3) pm)[6] and $[Al\{Me_2Si(NPh)_2\}_2]^-$ (172.8(2)–173.8(2) pm).[17] The formation of the $SiN_2Cr$ chelate rings leads to a marked reduction of the N–Si–N angle from 111.3(2)–112.0(2)° in $Me_2Si(NHPh)_2$ to 93.89(1)° in compound **1**. Regarding some conformational aspects, it is noticeable that the phenyl groups attached to N1 and N2 are nearly coplanar to the $SiN_2Cr$ ring with C6-C1-N1-Cr and C12-C7-N2-Cr torsion angles of −16.8(3) and 8.3(3)°, resp. The tilt angle between the $SiN_2Cr$ plane and the imidazoline-2-ylidene planes are 60.7(1) and 74.1(1)°.

The remaining complexes $[Mn\{Me_2Si(NPh)_2\}(^iPr_2Im)_2]$ (**2**), $[Fe\{Me_2Si(NPh)_2\}(^iPr_2Im)_2]$ (**3**), $[Co\{Me_2Si(NPh)_2\}(^iPr_2Im)_2]$ (**4**) and $[Zn\{Me_2Si(NPh)_2\}(^iPr_2Im)_2]$ (**5**) were found to crystallize in the tetragonal system. Compounds **2**, **4** and **5** crystallize in the space group $P4_1$ and in the case of the iron derivative **3** the enantiomorphic space group $P4_3$ was observed. The molecular structures of the abovementioned complexes are different from those of compound **1** in that way that the metal centers exhibit distorted tetrahedral coordination. In particular, this change in coordination mode has impacts on the C–M–C angles that are markedly larger than in the square planar derivatives.

The Mn derivative **2** (Figure 2) displays Mn–N distances of 208.8(5) pm and 209.2(5) pm. Slightly shorter distances were found for $[Mn\{N(SiMe_3)_2\}_2(py)_2]$ (205.9(1)–206.2(1) pm)[25] and $[Mn\{N(SiMe_3)_2\}_2(Bipy)]$ (203.5(1) pm).[26] $[Mn_2\{Me_2Si(NDipp)_2\}_2]$ exhibits Mn–N distances of 196.4(3) pm for the $\kappa^1$ coordinating N atom, 205.8(3) pm and 225.0(3) pm for the μ-N atom.[9] The Mn–C distances (218.8(5) and 220.8(5) pm) are within the expected range. A search in the CSD database[21] revealed a median Mn–C distance of 220.2 pm for Mn-NHC complexes (67 data, lower quantile: 218.4 ppm, upper quantile: 221.7 pm). Like in the case of the Cr(II) derivative, the formation of a four membered $SiN_2Mn$ chelate ring leads to an acute N–Mn-N angle of 75.0(2)°. The largest angle is formed by the C–Mn–C unit (117.8(2)°) and obviously this is favored by the steric repulsion of the bulky $^iPr_2Im$ ligands. The N–Mn–C angles are 110.7(2) to 116.6(2)° and in summary, the $\tau_4'$ parameter (0.89) reveals a moderately distorted tetrahedral coordination. The molecular structures of the related complexes $[Fe\{Me_2Si(NPh)_2\}(^iPr_2Im)_2]$ (**3**)

 

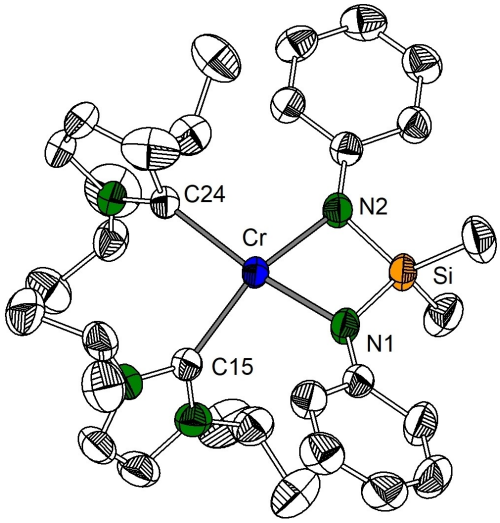


**Figure 1.** Molecular structure of compound **1**. Thermal ellipsoids at the 50 % level. For clarity H atoms were omitted. Selected bond lengths/distances (pm) and angles (°): Cr–N(1) 203.1(2), Cr–N(2) 204.9(2), Cr–C(15) 214.6(2), Cr–C(24) 214.4(2), Si–N(1) 170.9(2), Si–N(2) 172.8(2), Si–C(13) 186.8(3), Si–C(14) 188.0(3), N(1)–Cr–N(2) 75.98(6), N(1)–Cr–C(15) 95.14(7), N(1)–Cr–C(24) 166.94(8), N-(2)–Cr–C(15) 155.74(8), N(2)–Cr–C(24) 102.54(7), C(24)–Cr–C(15) 91.03(7), N(1)–Si–N(2) 93.89(8), N(1)–Si–C(13) 113.0(1), N-(1)–Si–C(14) 114.5(1), N(2)–Si–C(13) 116.5(1), N(2)–Si–C(14) 112.1(1), C(13)–Si–C(14) 106.8(3).

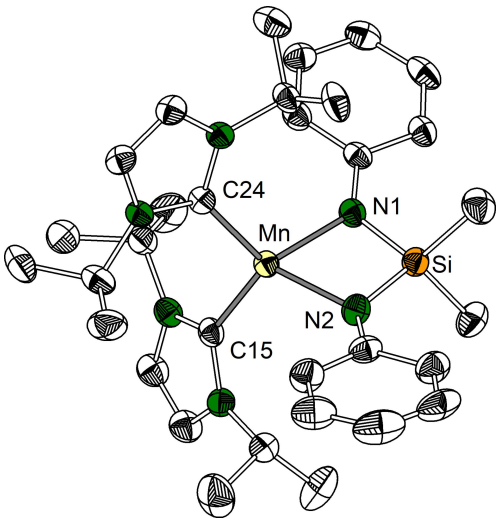


**Figure 2.** Molecular structure of compound **2**. Thermal ellipsoids at the 50 % level. For clarity H atoms were omitted. Selected bond lengths/distances (pm) and angles (°): Mn–N(1) 209.2(5), Mn–N(2) 208.8(5), Mn–C(15) 220.8(6), Mn–C(24) 218.8(5), Si(1)–N(1) 172.1(5), Si(1)–N(2) 171.4(5), Si(1)–C(13) 188.0(6), Si(1)–C(14) 188.5(6), N-(1)–Mn–C(15) 110.7(2), N(1)–Mn–C(24) 116.6(2), N(2)–Mn–N(1) 75.0(2), N(2)–Mn–C(15) 114.6(2), N(2)–Mn–C(24) 114.8(2), C(24)–Mn–C(15) 117.8(2), N(1)–Si–C(13) 113.4(3), N(1)–Si–C(14) 114.6(3), N(2)–Si–N(1) 95.6(2), N(2)–Si–C(13) 114.8(3), N(2)–Si–C(14) 112.6(3), C(13)–Si–C(14) 106.0(3).

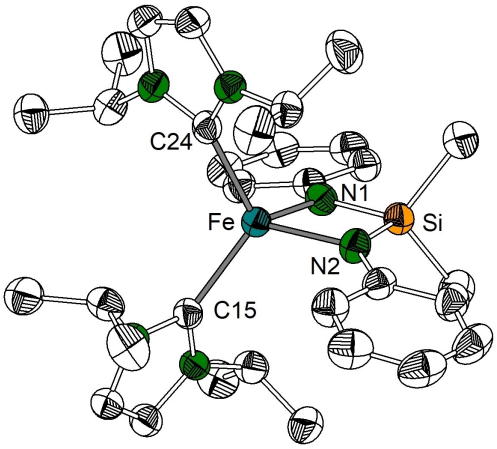


**Figure 3.** Molecular structure of compound **3**. Thermal ellipsoids at the 50 % level. For clarity H atoms were omitted. Selected bond lengths/distances (pm) and angles (°): Fe–N(1) 202.6(3), Fe–N(2) 202.2(3), Fe– C(15) 213.4(3), Fe–C(24) 213.1(3), Si–N(1) 172.1(3), Si–N(2) 172.3(3), Si–C(13) 187.6(4), Si–C(14) 188.3(4), N(1)–Fe–C(15) 116.5(1), N(1)–Fe–C(24) 111.5(1), N(2)–Fe–N(1) 77.6(1), N-(2)–Fe–C(15) 113.4(1), N(2)–Fe–C(24) 116.4(1), C(24)–Fe–C(15) 115.9(1), N(1)–Si–N(2) 94.9(1), N(1)–Si–C(13) 114.9(2), N(1)–Si–C(14) 114.0(2), N(2)–Si–C(13) 113.0(2), N(2)–Si–C(14) 114.9(2), C(13)–Si–C(14) 105.4(2).

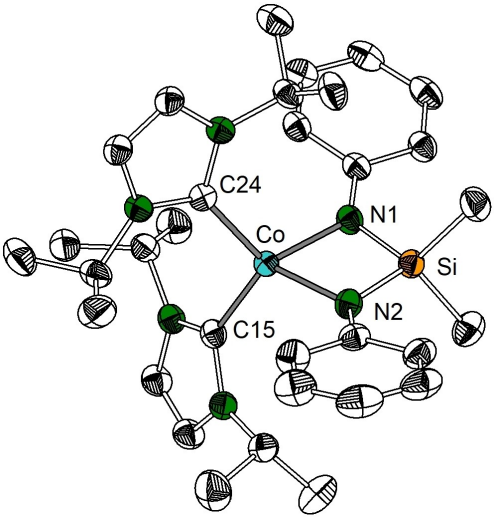


**Figure 4.** Molecular structure of compound **4**. Thermal ellipsoids at the 50 % level. For clarity H atoms were omitted. Selected bond lengths/distances (pm) and angles (°):Co–N(1) 200.8(2), Co–N(2) 200.4(2), Co–C(15) 207.8(2), Co–C(24) 207.2(2), Si–N(1) 171.9(2), Si–N(2) 171.7(2), Si–C(13) 187.8(3), Si–C(14) 187.9(3), N(1)–Co-C(15) 110.98(9), N(1)–Co–C(24) 117.17(9), N(2)–Co–N(1) 77.67(8), N-(2)–Co–C(15) 116.14(9), N(2)–Co–C(24) 113.46(9), C(24)–Co–C(15) 115.88(9), N(1)–Si–C(13) 114.3(1), N(1)–Si–C(14) 115.1(1), N(2)–Si–N-(1) 94.1(1), N(2)–Si–C(13) 115.1(1), N(2)–Si–C(14) 113.1(1), C(13)–Si–C(14) 105.3(1).

(Figure 3), [Co{$Me_2Si(NPh)_2$}($^iPr_2Im)_2$] (**4**) (Figure 4) and [Zn{$Me_2Si$-$(NPh)_2$}($^iPr_2Im)_2$] (**5**) (Figure 5) are very similar. The Fe–N bond lengths in **3** (202.2(3) and 202.6(2) pm) are just 7 pm shorter

 

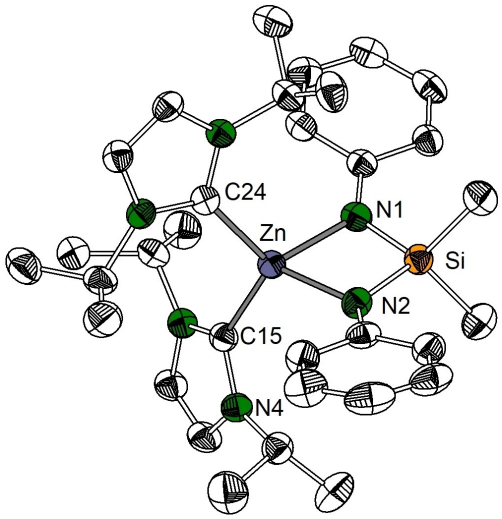


**Figure 5.** Molecular structure of compound **5.** Thermal ellipsoids at the 50 % level. For clarity H atoms were omitted. Selected bond lengths/distances (pm) and angles (°): Zn–N(1) 204.9(4), Zn–N(2) 203.8(4), Zn–C(15) 208.8(5), Zn–C(24) 207.4(5), Si–N(1) 171.5(4), Si–N(2) 172.2(4), Si–C(13) 188.2(6), Si–C(14) 188.2(6), N(1)–Zn–C(15) 110.67(18), N(1)–Zn–C(24) 117.0(2), N(2)–Zn–N(1) 76.5(2), N-(2)–Zn–C(15) 114.8(2), N(2)–Zn–C(24) 114.3(2), C(24)–Zn–C(15) 117.1(2), N(1)–Si–N(2) 94.8(2), N(1)–Si–C(13) 114.0(3), N(1)–Si–C(14) 115.1(2), N(2)–Si–C(13) 115.4(3), N(2)–Si–C(14) 113.0(3), C(14)–Si–C(13) 104.8(3)

than in the case of the manganese derivative **2**. In $[Fe_3\{Me_2Si(N\text{-}CH_2\text{-}o\text{-}py)_2\}_2Cl_2]$ the Fe–N distances are 199.6(4) and 199.8(4) pm for the tetracoordinated iron atoms and 205.3(4)–224.1(4) pm for the pentacoordinated iron atoms.[13] A further shortening around 2 pm is observed for the cobalt complex (200.4(2) and 200.8(2) pm). The Co–N distances found in $[Co\{Me_2Si(NtBu)_2\}_2]$ are much shorter with 183.7(1) to 184.3(1) pm.[5] In the case of the zinc complex **5**, the Zn–N bond lengths (203.8(4) and 204.9(4) pm) are slightly larger than the Fe–N distances in **3**. In $[Zn_2\{Me_2Si(NDipp)_2\}_2]$ with linearly coordinated Zn atoms the Zn–N distances are significantly shorter (181.2(3)–182.8(3) pm) and in $K_2[Zn_2\{Me_2Si(NDipp)_2\}_2]$ that contains chelating $Me_2Si(NDipp)_2^{2-}$ ligands the Zn–N distances (202.2–203.0 pm) are close to those in compound **5**.[27] $[Zn_2\{Ph_2Si(NR')_2\}_2]$ (R = 8-quinolyl) with tetracoordinated Zn atoms exhibits Zn–N distances in a medium range (195.6(3)–197.7(4) pm).[14] The metal-C distances follow a similar tendency as the metal-N distances. The iron derivative **3** exhibits Fe–C distances of 213.1(3) and 213.4(3) pm that are around 7 pm shorter than the Mn–C distances and a further reduction of approx. 6 pm is found for the Co–C distances in complex **4** (207.2(2) and 207.8(2) pm). The Zn–C distances in compound **5** (207.4(5) and 208.8(5) pm) are slightly larger than in the Co derivative **4**. According to a CSD search,[21] Fe–C distances in Fe-NHC complexes with coordination number 4 vary from 192.2–221.0 pm with a median value of 208.4 pm (361 data, lower quantile 203.5 pm, upper quantile 211.4 pm). In the case of analogous Co-NHC complexes the range is 175.9–208.9 pm with a median of 197.3 pm (251 data, lower quantile 192.7 pm, upper quantile 202.6 pm). Moreover, the Zn–C distances in Zn-NHC complexes vary from 190.3–215.9 pm with a median of 204.0 pm (90 data, lower quantile 202.0 pm, upper quantile 206.4 pm). Regarding the bond angles around the central metal atoms, there are no larger differences for the Fe, Co and Zn derivative in comparison with the Mn compound **2**. There are always acute N–M–N angles (M = Fe (77.6(1)°), Co (77.7(1)°), 76.5(2)°) due to the presence of four-membered $SiN_2M$ chelate rings and relatively large C–M–C angles (M = Fe (115.9(1)°), Co (115.9(1)°), Zn 117.1(2)°) as a result of steric hindrance of the bulky NHC ligands. The similarity of the distortions is also evident from the $\tau_4'$ parameters (0.90 (Fe), 0.89 (Co, Zn)). Concerning the geometrical parameters of the $Me_2Si(NPh)_2$ group there is only neglectable influence of the coordinated metal atoms on the Si–N distances and N–Si–N angles (Table 2).

## Conclusion

A series of five complexes $[M\{Me_2Si(NPh)_2\}(^iPr_2Im)_2]$ (M = Cr, Mn, Fe, Co, Zn) were synthesized in order to study the coordination behavior of the $Me_2Si(NPh)^{2-}$ ligands towards different divalent 3d metals. The syntheses were carried out in the presence of the NHC ligand $^iPr_2Im$ in order to enhance the kinetic stability of

**Table 2.** Selected bond lengths/distances (pm) and angles for compounds **1**–**5**.

| | **1** (M = Cr) | **2** (M = Mn) | **3** (M = Fe) | **4** (M = Co) | **5** (M = Zn) |
|---|---|---|---|---|---|
| M–C15 | 214.6(2) | 220.8(6) | 213.4(3) | 207.8(2) | 208.8(5) |
| M–C24 | 214.4(2) | 218.8(5) | 213.1(3) | 207.2(2) | 207.4(5) |
| M–N1 | 203.1(2) | 209.2(5) | 202.6(3) | 200.8(2) | 204.9(4) |
| M–N2 | 204.9(2) | 208.8(5) | 202.2(3) | 200.4(2) | 203.8(4) |
| Si–N1 | 170.9(2) | 172.1(5) | 172.1(3) | 171.9(2) | 171.5(4) |
| Si–N2 | 172.8(2) | 171.4(5) | 172.3(3) | 171.7(2) | 172.2(4) |
| N–M–N | 75.98(6) | 75.0(2) | 77.6(1) | 77.67(8) | 76.5(2) |
| C–M–C | 91.03(7) | 117.8(2) | 115.9(1) | 115.88(9) | 117.1(2) |
| Si–N1–M | 95.12(8) | 94.5(2) | 93.62(12) | 93.93(10) | 94.18(19) |
| Si–N2–M | 93.91(7) | 94.9(2) | 93.72(13) | 94.12(10) | 94.36(19) |
| N–Si–N | 93.89(8) | 95.6(2) | 94.9(1) | 94.1(1) | 94.8(2) |
| $\tau_4'$-parameter[22] | 0.23 | 0.89 | 0.90 | 0.89 | 0.89 |

 

the products and to prevent oligomerization reactions. However, the complexes are still extremely air and moisture sensitive. The determination of the molecular structures of compounds **1**–**5** confirmed the expected square planar coordination for Cr(II) ($d^4$ configuration) and tetrahedral coordination for Mn(II), Fe(II), Co(II) and Zn(II). Future investigations will be dedicated to the synthesis of analogous $d^8$ configurated Ni(II), Pd(II) and Pt(II) derivatives which also should display square planar coordination. Moreover, the redox properties of the Cr(II), Mn(II), Fe(II) and Co(II) complexes deserve further attention.

## Experimental Section

**General**: All experiments were carried out using common Schlenk techniques under an argon atmosphere in flame dried glass ware. All solvents were dried over sodium/benzophenone and freshly distilled prior to use. Air and moisture were excluded rigorously.

NMR spectra were recorded on a VARIAN Inova 500 spectrometer ($^1$H, 500 MHz; $^{13}$C, 125 MHz; $^{29}$Si, 100 MHz) at 25 °C. Chemical shifts for $^1$H and $^{13}$C were referred relative to the solvent. All $^{13}$C and $^{29}$Si spectra have been broad-band decoupled, additionally all $^{29}$Si spectra were carried out as INEPT. THF-$D_8$ was freshly distilled from sodium potassium alloy (23 % Na, 77 % K). IR spectra were recorded on a Bruker Tensor 2 equipped with a diamond ATR unit.

Due to extreme moisture and air sensitivity compounds **1**–**5** were not suitable for elemental analysis. For analysis the metal contents were determined photometrically. Fe and Co were determined as thiocyanate complexes,[28] Cr as chromate[29] and zinc as dithizone complex.[29]

Magnetic measurements were carried out at room temperature with a Johnson-Matthey Evans balance.

The compounds $[Cr_2(OAc)_4]$,[30] [M(acac)$_2$(TMEDA)] (M = Mn, Fe, Co, Zn),[31] $Me_2Si(NHPh)_2$[32] and $^iPr_2Im$[33] were prepared according to literature methods.

## X-ray Structure Determination

Single crystals of the complexes were investigated by a STOE IPDS 2 (**1**, **3**, **4**, **5**) and a STOE I2T diffractometer (**2**), using Mo-$K_\alpha$ radiation ($\lambda$ = 0.71073 Å).

X-Area software was used to evaluate and integrate the diffraction data. SHELXT[34] was applied to solve the structures and refinement was done with SHELXL against $F^2$,[35] using OLEX$^2$ as graphical interface.[36] Graphical representations of the crystal structures were created with the Diamond software.[37] All hydrogen atoms have been placed geometrically riding on their carbon atoms with displacement parameters $U_{iso}$(H) = 1.5 $U_{eq}$(C) for methyl groups or $U_{iso}$(H) = 1.2 $U_{eq}$(C) otherwise.

Crystallographic data have been deposited with the Cambridge Crystallographic Data Centre. Copies of these data can be obtained free of charge from the Cambridge Crystallographic Data Centre on application to the Director, CCDC, 12, Union Road, Cambridge CB2 1 EZ, UK (e-mail: deposit@ccdc.cam.uk).

## Synthesis of [M{$Me_2Si(NPh)_2$}($^iPr_2Im$)$_2$]

The complexes **1** to **5** were prepared by adding $^iPr_2Im$ (1.67 g, 11 mmol) to a stirred suspension or solution of $[Cr_2(OAc)_4]$ (2.5 mmol) or [M(acac)$_2$TMEDA] (M = Mn, Fe, Co, Zn; 5 mmol)) at room temperature. This led to different changes in color depending on M. The red suspension of $[Cr_2(OAc)_4]$ turned into a violet solution. The solution stayed red for Fe. In the case of Mn and Zn the color changed from yellow to orange and for Co from red to brown. Afterwards a THF solution of $Li_2Me_2Si(NPh)_2$ which was freshly prepared from $Me_2Si(NHPh)_2$ (1.21 g, 5 mmol) and *n*-butyllithium (2 ml, 2.5 M in *n*-hexane) was added at −70 °C. After warming to room temperature, the solutions were stirred overnight. THF was removed in vacuo and the residue was extracted with hot toluene (40 ml). The products **1**–**5** were precipitated from the toluene extract at room temperature as microcrystalline solids.

Single crystals suitable for X-ray diffraction analysis were obtained by cooling down a dimethoxyethane (Mn), or *o*-xylene (Cr) solution of the complex or by slow diffusion of *n*-hexane in a THF solution (Fe, Co, Zn).

### *[Cr{$Me_2Si(NPh)_2$}($^iPr_2Im$)$_2$] (1)*

Red crystals, yield: 1.76 g (59 %). $C_{32}H_{48}CrN_6Si$ (596.85 g/mol): Cr 8.5 (calc. 8.7)%; **IR**: 3155 w, 3125 w, 3067 m, 3023 m, 2965 m, 2935 m, 2872 m, 1668 m, 1601 m, 1583 s, 1487 m, 1476 s, 1424 m, 1416 m, 1392 m, 1371 m, 1332 m, 1295 s, 1260 s, 1239 m, 1207 s, 1172 m, 1131 m, 1106 m, 1071 m, 1024 m, 989 m, 957 m, 929 m, 914 m, 898 m, 875 m, 835 s, 785 s, 766 s, 751 s, 730 s, 689 s, 629 m, 617 m, 595 m, 583 m, 565 m, 512 s, 465 m, 429 m, 413 m, 396 m, 382 m, 372 m, 360 m, 328 m, 305 s, 247 m, 222 m, 210 m cm$^{-1}$.

UV/vis (THF): $\lambda_{max}$ ($\varepsilon$/mol$^{-1}$cm$^{-1}$) = 243 (1975000), 291 (705000), 487 (370) nm.

Suitable crystals for X-ray diffraction were obtained from hot *o*-xylene.

### *[Mn{$Me_2Si(NPh)_2$}($^iPr_2Im$)$_2$] (2)*

Colorless crystals, yield: 1.74 g (58 %). $C_{32}H_{48}MnN_6Si$ (599.79 g/mol): Mn 9.1 (calc. 9.2) **IR**: 3164 w, 3138 w, 3127 w, 3057 w, 3010 w, 2972 m, 2931 m, 2875 w, 1604 w, 1577 m, 1550 m, 1480 s, 1463 m, 1420 w, 1406 m, 1391 m, 1371 m, 1311 s, 1265 m, 1229 m, 1206 m, 1166 m, 1144 m, 1131 m, 1105 m, 1068 m, 1022 m, 987 m, 955 w, 925 s, 881 m, 855 m, 823 m, 789 m, 747 s, 732 s, 693 m, 671 m, 658 m, 615 m, 605 m, 580 m, 561 m, 516 m, 412 m, 375 m, 354 m, 284 m, 251 m, 230 m, 212 m cm$^{-1}$.

### *[Fe{$Me_2Si(NPh)_2$}($^iPr_2Im$)$_2$] (3)*

Yellow crystals, yield: 1.83 g (61 %). $C_{32}H_{48}FeN_6Si$ (600.69 g/mol): Fe 9.3 (calc. 9.3)%. **IR**: 3166 w, 3138 m, 3127 w, 3058 m, 3013 m,

 

2972 m, 2931 m, 2874 m, 2652 m, 2532 w, 1577 m, 1480 s, 1463 m, 1447 m, 1419 m, 1405 m, 1390 m, 1370 m, 1305 s, 1267 m, 1230 m, 1206 s, 1165 m, 1146 m, 1131 m, 1106 m, 1068 m, 1022 m, 988 s, 957 w, 925 s, 880 m, 860 m, 824 m, 788 m, 749 s, 736 m, 728 s, 693 m, 671 m, 616 m, 586 m, 561 m, 516 m, 412 m, 375 m, 355 m, 309 m, 285 m, 277 m, 252 m, 227 m, 211 m $cm^{-1}$.

UV/vis (THF): $\lambda_{max}$ ($\varepsilon$/$mol^{-1}cm^{-1}$) = 245 (1609000), 290 (532000), 412 (2490) nm, 472 (1270) nm.

### *[Co{$Me_2Si(NPh)_2$}($^iPr_2Im)_2$] (4)*

Green crystals, yield: 1.89 g (63 %). $C_{32}H_{48}CoN_6Si$ (603.78 g/mol): Co 9.6 (calc. 9.8)%. **IR**: 3169 w, 3139 m, 3128 w, 3095 w, 3059 m, 2972 m, 2932 m, 2875 m, 2662 w, 2535 w, 1606 w, 1577 m, 1480 s, 1463 s, 1447 m, 1420 m, 1406 m, 1391 m, 1370 m, 1305 s, 1269 m, 1230 m, 1206 s, 1165 m, 1132 m, 1106 m, 1068 m, 1022 m, 988 s, 957 m, 942 m, 927 s, 880 m, 860 m, 854 m, 825 m, 787 m, 750 s, 730 s, 694 m, 674 m, 660 m, 616 m, 585 m, 562 m, 515 m, 457 m, 414 m, 379 m, 356 m, 300 m, 250 s, 215 m $cm^{-1}$.

UV/vis (THF): $\lambda_{max}$ ($\varepsilon$/$mol^{-1}cm^{-1}$) = 245 (2138000), 290 (758000), 444 (2110), 614 (1370), 689 (460) nm.

### *[Zn{$Me_2Si(NPh)_2$}($^iPr_2Im)_2$] (5)*

Colorless crystals, yield: 1.98 g (65 %). $C_{32}H_{48}CrN_6Si$ (596.85 g/mol): Zn 11.1 (calc. 10.7)%; **IR**: 3168 w, 3139 w, 3128 w, 3058 w, 2973 w, 2930 w, 2876 w, 1604 w, 1578 m, 1552 w, 1541 w, 1514 w, 1481 s, 1463 m, 1411 m, 1393 m, 1375 m, 1318 s, 1268 m, 1229 m, 1207 m, 1167 m, 1132 w, 1109 m, 1068 w, 1022 m, 987 m, 942 m, 930 s, 881 m, 856 m, 824 m, 788 m, 748 m, 735 s, 695 m, 671 m, 656 m, 614 m, 604 m, 580 m, 562 m, 515 m, 415 m, 378 m, 355 m, 311 w, 268 m, 244 m, 227 m, 214 m $cm^{-1}$.

**$^1$H NMR** (500 MHz, THF-$D_8$) δ 7.35 (s, 4H, N-C*H*-C*H*-N), 6.71 – 6.63 (m, 4H, $CH_{Ar}$), 6.24–6.18 (m, 4H, $CH_{Ar}$), 5.97 (m, 2H, *p*-$CH_{Ar}$), 5.13 (hept, J = 6.6 Hz, 4H, N-C*H*), 1.23 (d, J = 6.7 Hz, 24H, CH-$CH_3$), 0.17 (s, 6H, Si-$CH_3$).

**$^{13}$C NMR** (125 MHz, THF-$D_8$) δ 176.7, 158.1, 127.7, 119.1, 117.1, 108.9, 51.5, 22.7, 0.9.

**$^{29}$Si NMR** (100 MHz, THF-$D_8$) δ −15.8.

## Acknowledgements

This work was supported by a scholarship of the state of Saxony-Anhalt (Graduiertenförderungsgesetz) Open Access funding enabled and organized by Projekt DEAL.

## Conflict of Interest

The authors declare no conflict of interest.

## Data Availability Statement

The data that support the findings of this study are available from the corresponding author upon reasonable request.

**Keywords:** Silylamide · Carbene ligands · Crystal Structure · X-ray diffraction

[1] M. Lappert, A. Protchenko, P. Power, A. Seeber, *Metal amide chemistry*, Wiley, Chichester, U.K **2009**.
[2] W. D. Beiersdorf, D. J. Brauer, H. Brger, *Z. Anorg. Allg. Chem.* **1981**, *475*, 56–66.
[3] D. J. Brauer, H. Bürger, E. Essig, W. Geschwandtner, *J. Organomet. Chem.* **1980**, *190*, 343–351.
[4] D. J. Brauer, H. Bürger, G. R. Liewald, J. Wilke, *J. Organomet. Chem.* **1986**, *310*, 317–332.
[5] D. Zanders, G. Bačić, D. Leckie, O. Odegbesan, J. Rawson, J. D. Masuda, A. Devi, S. T. Barry, *Angew. Chem. Int. Ed.* **2020**, *59*, 14138–14142; *Angew. Chem.* **2020**, *132*, 14242–14246.
[6] C. Wagner, K. Merzweiler, *Z. Anorg. Allg. Chem.* **2014**, *640*, 2198–2202.
[7] P. Liebing, K. Merzweiler, *Z. Anorg. Allg. Chem.* **2022**, *648*.
[8] H. Chen, R. A. Bartlett, H. V. R. Dias, M. M. Olmstead, P. P. Power, *Inorg. Chem.* **1991**, *30*, 2487–2494.
[9] D.-Y. Lu, J.-S. K. Yu, T.-S. Kuo, G.-H. Lee, Y. Wang, Y.-C. Tsai, *Angew. Chem. Int. Ed.* **2011**, *50*, 7611–7615; *Angew. Chem.* **2011**, *123*, 7753–7757.
[10] Y.-C. Tsai, Y.-M. Lin, J.-S. K. Yu, J.-K. Hwang, *J. Am. Chem. Soc.* **2006**, *128*, 13980–13981.
[11] P. Mastropierro, Z. Livingstone, S. D. Robertson, A. R. Kennedy, E. Hevia, *Organometallics* **2020**, *39*, 4273–4281.
[12] P. Mastropierro, A. R. Kennedy, E. Hevia, *Eur. J. Inorg. Chem.* **2021**, *2021*, 1016–1022.
[13] A. Malassa, B. Schulze, B. Stein-Schaller, H. Görls, B. Weber, M. Westerhausen, *Eur. J. Inorg. Chem.* **2011**, *2011*, 1584–1592.
[14] A. Malassa, C. Koch, B. Stein-Schaller, H. Görls, M. Friedrich, M. Westerhausen, *Inorg. Chim. Acta* **2008**, *361*, 1405–1414.
[15] R. Albrecht, P. Liebing, U. Morgenstern, C. Wagner, K. Merzweiler, *Z. Naturforsch. B* **2019**, *74*, 233–240.
[16] J. Pikies, W. Wojnowski, *Z. Anorg. Allg. Chem.* **1985**, *521*, 173–182.
[17] A. Mane, C. Wagner, K. Merzweiler, *Z. Anorg. Allg. Chem.* **2012**, *638*, 136–140.
[18] Y.-F. Deng, T. Han, Z. Wang, Z. Ouyang, B. Yin, Z. Zheng, J. Krzystek, Y.-Z. Zheng, *Chem. Commun.* **2015**, *51*, 17688–17691.
[19] W. Zhou, A. N. Desnoyer, J. A. Bailey, B. O. Patrick, K. M. Smith, *Inorg. Chem.* **2013**, *52*, 2271–2273.
[20] S. N. König, C. Schädle, C. Maichle-Mössmer, R. Anwander, *Inorg. Chem.* **2014**, *53*, 4585–4597.
[21] C. R. Groom, I. J. Bruno, M. P. Lightfoot, S. C. Ward, *Acta Crystallogr., Sect. B: Struct. Sci., Cryst. Eng. Mater.* **2016**, *72*, 171–179.
[22] $\tau_4' = \frac{\beta-\alpha}{360°-\theta} + \frac{180°-\beta}{180°-\theta}$ ($\beta > \alpha$; $\theta = \cos^{-1}(-1/3)$). A. Okuniewski, D. Rosiak, J. Chojnacki, B. Becker, *Polyhedron* **2015**, *90*, 47–57.
[23] H.-L. Dong, H.-B. Tong, X.-H. Wei, S.-P. Huang, D.-S. Liu, *Acta Crystallogr., Sect. E: Struct. Rep. Online* **2005**, *61*, o1354-o1355.
[24] L. Zhou, Y. Yao, C. Li, Y. Zhang, Q. Shen, *Organometallics* **2006**, *25*, 2880–2885.
[25] A. Panda, M. Stender, M. M. Olmstead, P. Klavins, P. P. Power, *Polyhedron* **2003**, *22*, 67–73.
[26] C. R. Hamilton, M. R. Gau, R. A. Baglia, S. F. McWilliams, M. J. Zdilla, *J. Am. Chem. Soc.* **2014**, *136*, 17974–17986.
[27] Y.-C. Tsai, D.-Y. Lu, Y.-M. Lin, J.-K. Hwang, J.-S. K. Yu, *Chem. Commun.* **2007**, 4125–4127.

 

[28] R. E. Kitson, *Anal. Chem.* **1950**, *22*, 664–667.
[29] B. Lange, Z. J. Vejdělek, *Photometrische Analyse*, 1st ed., VCH, Weinheim, New York, NY **1987**.
[30] M. D. Hartle, J. S. Prell, M. D. Pluth, *Dalton Trans.* **2016**, *45*, 4843–4853.
[31] J. H. Halz, C. Heiser, C. Wagner, K. Merzweiler, *Acta Crystallogr., Sect. E: Crystallogr. Commun.* **2020**, *76*, 66–71.
[32] K. Kraushaar, M. Herbig, D. Schmidt, J. Wagler, U. Böhme, E. Kroke, *Z. Naturforsch. B* **2017**, *72*, 909–921.
[33] O. V. Starikova, G. V. Dolgushin, L. I. Larina, T. N. Komarova, V. A. Lopyrev, *Arkivoc* **2003**, *2003*, 119–124.
[34] G. M. Sheldrick, *Acta Crystallogr., Sect. A: Found. Adv.* **2015**, *71*, 3–8.
[35] G. M. Sheldrick, *Acta Crystallogr. Sect. C* **2015**, *71*, 3–8.
[36] O. V. Dolomanov, L. J. Bourhis, R. J. Gildea, J. A. K. Howard, H. Puschmann, *J. Appl. Crystallogr.* **2009**, *42*, 339–341.
[37] H. Putz, K. Brandenburg, *Diamond – Crystal and Molecular Structure Visualization*, Crystal Impact, Bonn, Germany **1996**.
[38] S. Parsons, H. D. Flack, T. Wagner, *Acta Crystallogr., Sect. B: Struct. Sci., Cryst. Eng. Mater.* **2013**, *69*, 249–259.

Manuscript received: July 25, 2022
Revised manuscript received: August 30, 2022

 